

## BIOMIMETIC FABRICATION OF MATERIALS-THE MINIMALIST APPROACH

Joydeep Lahiri, Guofeng Xu, Tu Lee, Daniel M. Dabbs, Nan Yao, Ilhan A. Aksay and John T. Groves\*

Department of Chemistry and the Princeton Materials Institute  
Princeton University  
Princeton, NJ 08544

### ABSTRACT

The interfacial chemistry between inorganic ceramics and defined organic surfaces is the focus of intense investigation.

Partially compressed Langmuir-Blodgett monolayers of anionic porphyrins have been used as modified nucleation sites for calcium carbonate. The porphyrin monolayer has an ordered array of carboxylates, and hence the system serves as a minimalist template for the modeling of complex biogenic acidic glycoproteins for biomineralization. The initial results suggest the formation of calcite with morphologically distinct calcitic rhombs with truncated, 3-edged corners and intricately articulated facial cavities. Stearic acid monolayers yield distinctly different calcite crystals, indicative that the geometrically defined carboxylate array is probably important.

Phosphatidylcholine vesicles have been used as a tool for the formation of membrane encapsulated iron-oxides. Gramicidin A ion channels have been embedded in vesicles to kinetically alter the formation and growth of iron oxides, starting with intravesicular ferrous chloride. The results indicate that the presence of ion channels lead to the formation of magnetite vis-a-vis maghemite formation in vesicles lacking the ion channels. The use of ion channels has important implications in probable signal transduction processes during biomineralization pathways.

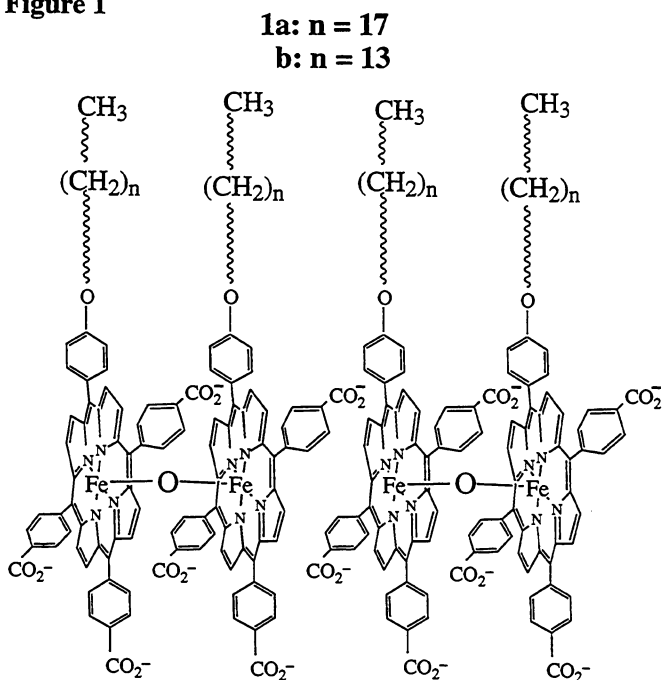
### INTRODUCTION

Inorganic materials in living organisms are formed by controlled crystallization on protein and glycosidic matrices. Understanding the chemical and molecular principles of such biomineralization processes has been the focus of intense research both to derive an understanding of the biochemistry for the growth of mesoscopic structures and as an inspiration to devise new strategies for materials fabrication.<sup>1</sup> Organisms are able to manipulate their cellular machinery to develop uniquely architected inorganic materials for a variety of functions, and hence, biological systems constitute an important inspirational source for the design and processing of novel ceramics.<sup>1</sup> The importance of epitaxy and stereochemical control as determinants in the symmetry and growth of the crystals has been widely discussed.<sup>1</sup> However, model studies using small molecules as templates for nucleation has failed to explain the morphological control mechanisms and numerous subtleties associated with biogenic protein templates. We have sought to design organic, amphiphilic templates that are of a complexity intermediate between protein matrices and simple molecules such as stearic acid. This approach could help delineate the effects of cooperativity<sup>2</sup>, spatial-stereochemical effects<sup>3</sup>, and especially help determine what minimal structure is required to mimic the controlled nucleation observed in biological systems.

We have described novel anionic, amphiphilic tricarboxyphenyl hemes that are able to recruit the peripheral membrane protein cytochrome c to the membrane surface. This occurs via the electrostatic interactions between its carboxylates and the positively charged lysine patch on the cytochrome c.<sup>8</sup> Monolayer techniques and spectroscopic evidence have indicated that the heme macrocycle is oriented perpendicular to the lipid-water interface. The m-oxo iron(III) porphyrin dimer (**1**) of these trianionic amphiphiles would thus provide 6-carboxylate groups in a semi-rigid array affording potential nucleation sites for cationic surfaces in crystals. We describe here the nucleation of calcite crystals on a compressed

monolayer surface of the template iron porphyrin dimer **1**.<sup>9</sup> The polycarboxylate cluster of this tricarboxy porphyrin yielded calcite crystals that were attached to the amphiphilic surface by a corner of the calcite rhombohedron, very similar to the result for the mollusk glycoproteins.<sup>2</sup> Further, a significant number of these crystals displayed intricately articulated cavities reminiscent of the laminations observed in these biogenic structures.

**Figure 1**



One of the most outstanding examples of biological materials-processing is the formation of magnetite in certain bacteria for navigational purposes. In several of these 'magnetotactic' organisms, magnetite particles referred to as magnetosomes, occur within vesicles consisting of phospholipid bilayers.<sup>2</sup> However, the control mechanisms whereby mono-disperse, single crystal, single domain magnetite particles are formed is still unclear, and signal transduction processes have been implicated. The use of gated ion channels for modulation of crystal growth constitutes an interesting, though speculative signal transduction pathway. It is noteworthy that ferritin, the principal iron-storage protein in mammals and other organisms, has ion-channels that facilitate the movement of iron across the approximately spherical protein shell. We have used gramicidin A (gma) ion

channels in phospholipid vesicles to control the phase and particle size of iron-oxide.

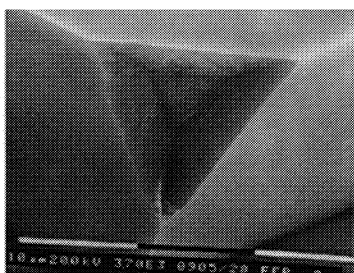
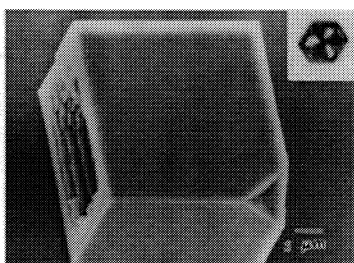
## ANIONIC PORPHYRIN TEMPLATES AS NUCLEATION SITES FOR CALCIUM CARBONATE

Calcium carbonate minerals are prevalent in a wide variety of organisms<sup>4</sup> serving diverse functions as exoskeletons, eye lenses, spicules etc. and having defined ultrastructures to meet their functional requirements. One of the predominant polymorphs is calcite which is characterized by alternating layers of calcium and carbonate ions aligned perpendicular to the crystallographic *c* axis, with the planar carbonate lying in the *ab* plane. Addadi and Weiner have shown that acidic glycoproteins from the mollusk shell are able to induce oriented {0 0 . 1} nucleation of calcite<sup>2, 5</sup> and have attributed this selectivity to cooperative sulfonate-carboxylate interactions in these  $\beta$ -sheet proteins.<sup>2</sup> However, sea urchin proteins specifically adsorb onto {1 -1 . 0} planes of calcite, which correspond to a bidentate orientation of the carbonate anions. Heywood and Mann have used stearic acid monolayers to nucleate the {1 -1 . 0} planes of calcite<sup>6</sup>, and have attributed the stereochemical match between its carboxylate oxygens and the bidentate orientation of the carbonate in this plane to override the epitaxial match of the (0 0 . 1) face. A third approach reported recently by Charych<sup>7</sup> has employed rigid polyacetylene templates to induce calcite alignment along the polymer backbone.

Calcium carbonate crystallites were grown at a water-amphiphile interface from supersaturated calcium bicarbonate solutions as described by Mann.<sup>6, 10</sup> The total Ca concentration was estimated by EDTA titrimetric analysis to be  $\sim 9 \text{ mmol dm}^{-3}$ . Monolayers of **1** were formed at the air/water interface using a solution of **1** in 3:1 chloroform/methanol (1mg/mL) to spread the film. The Langmuir monolayers

were compressed to 20-25 mN/m for all experiments. Isotherms were obtained by compression, and the limiting areas obtained were  $56 \text{ \AA}^2/\text{molecule}$  for **1** as compared to  $23 \text{ \AA}^2/\text{molecule}$  for stearic acid (Figure 1) under similar conditions. The limiting area obtained for **1** is close to that for vertically oriented tetraphenyl porphyrins ( $\sim 70 \text{ \AA}^2/\text{molecule}$ )<sup>11</sup> at air-water interfaces.

Calcium carbonate crystals were obtained by the slow, spontaneous loss of  $\text{CO}_2$  from the unstirred bicarbonate solutions. Crystals were studied by *in-situ* optical microscopy and SEM. SEM samples were prepared on microscope cover slips and mounted on stainless steel stubs using conducting carbon tape. Transfer of oriented  $\text{CaCO}_3$  crystals was accomplished by either dipping the cover slips through the films followed by withdrawal, or by briefly skipping the surface, following established procedures.<sup>6</sup> The dipping technique enables crystals to be viewed from above while the latter corresponds to viewing the crystals from the underside. Calcite was obtained as the predominant polymorph for nucleation by the porphyrin dimer **1** as it was for stearic acid<sup>12</sup> (see Figure 2, c-d), although 5-10% (by number) of the crystals in the former were vaterite.



*In-situ* optical microscopy viewed from above the porphyrin (**1**) monolayer revealed calcite crystals that were hexagonal in projection, indicative of their attachment to the amphiphilic surface by a truncated corner, presumably comprising the  $\{00.1\}$  face, as shown in Figure 2a (inset). Approximately 80 % of the crystals had this structural feature. Superficially, these truncations appeared to be flat. However, SEM images revealed that these corners consisted of three symmetry related  $\{10.2\}$  faces at  $120^\circ$  to each other. Figure 2a shows an SEM image of one such calcite crystal, obtained using the 'dipping' method.<sup>13</sup> The crystals have smooth rhombohedral  $\{10.4\}$  side faces and a symmetrical, concave depression at the surface attachment point. Interestingly,  $\sim 20\%$  of the three symmetry related distal  $\{10.4\}$  side faces had pronounced rectangular cavities, and some had two or three cavities on adjoining distal  $\{10.4\}$  faces. Distinct varieties of  $\{10.4\}$  cavities could be discerned. Some had layered and terraced galleries such as depicted in Figure 2a and others had bundles of rectangular projections as shown in Figure 2b. Both sets of features were approximately 1  $\mu\text{m}$  in size. Significantly, the crystals with a layered excavation on one  $\{10.4\}$  face had rectangular projections on the other face, suggesting different views of the same internal structure and producing an intrinsically chiral morphology even though calcite has a non-enantiomorphic crystal lattice. Viewed from the underside, the crystals had smooth basal  $\{10.4\}$  planes and  $\{10.4\}$  side faces with cavities, but the edges of the basal plane had no corner truncations.

We suggest that nucleation of these crystals occurred at or near the surface on the  $\{00.1\}$  face. The concave depression and the exposed  $\{10.2\}$  faces could be due either to inhibition of that face by the adsorbed porphyrin carboxylate cluster or limited diffusion of calcium ions to the truncated face due to the surface attachment.<sup>2</sup> There is also an interesting epitaxial match between the porphyrin template **1** and the  $\{10.2\}$  plane, which consists of a rectangular array of  $\text{Ca}^{2+}$ , with Ca-Ca distances of 4.99  $\text{\AA}$  and 9.98  $\text{\AA}$ . Molecular modeling indicates that the m-oxo dimer (**1**) has two  $\text{COO}^- - \text{COO}^-$  distances of  $\sim 5 \text{ \AA}$  and 10  $\text{\AA}$ , as shown<sup>14</sup>. It is possible that the result of two favorable epitaxial matches is responsible for nucleation on this face, and overrides the stereochemical mismatch of the  $\{1-1.0\}$  face. Various aspects of the nucleation and evolution of these crystals is currently under way.

The use of synthetic structurally defined polyanionic templates is an important approach towards an understanding of protein mediated crystal nucleation. The complexity of protein matrices precludes a thorough understanding of the different structural features responsible for control over crystal phase, morphology and growth. Hence, similar polyanionic templates (with systematic variation) could delineate the structural features required for the synergistic cooperative effects prevalent in biomineralization.

## MODULATION OF INTRAVESICULAR CRYSTAL GROWTH USING GRAMICIDIN ION CHANNELS

GmA is a naturally occurring pentadecapeptide which in its channel conformation exists as a head-to-head dimer spanning a lipid bilayer ( $\sim 40$  Å) with b-helical configuration.<sup>4</sup> It is a passive ion channel, i.e., it allows ions to flow freely in either direction according to the concentration gradient. Conductance studies have revealed that it conducts only monovalent cations with the following relative selectivities:  $\text{H}^+$  (150) >  $\text{NH}_4^+$  (8.9) >  $\text{Cs}^+$  (5.8) >  $\text{Rb}^+$  (5.5) >  $\text{K}^+$  (3.9) >  $\text{Na}^+$  (1.0) >  $\text{Li}^+$  (0.33).<sup>5</sup>

Vesicles have been used for the intravesicular mineralization of iron-oxides,<sup>6a</sup> cadmium and zinc sulfides,<sup>6b</sup> calcium phosphate<sup>6c</sup> etc. The ability of lipid based assemblies<sup>7</sup> to control the size and location of minerals constitutes a flexible approach towards mineralization.<sup>8</sup> Control may be achieved by regulation of headgroup structure, supersaturation, ionic strength, pH, temperature and various other factors. The use of ion channels offers an important new regulatory element, with possible control over particle size and accessibility to kinetic phases of minerals, especially when a balance of prototropy, ion influx/efflux and redox chemistry is desired.

Dimyristoyl phosphatidylcholine (DMPC) vesicles were formed by sonication of thin films of the lipid in the presence of *ferrous* chloride. For the preparation of vesicles doped with gmA, the lipid was co-dissolved with gmA in 2, 2, 2-trifluoroethanol (TFE) for thin film preparation.<sup>9</sup> Extravesicular  $\text{Fe}^{2+}$  ions were removed by passing it through a cation exchange resin for replacement by inert  $\text{Na}^+$  ions.<sup>10</sup> The coelution of the gmA peptide with the vesicles was confirmed by monitoring the u.v.-vis absorption spectrum of the eluting fractions.

It was important to ascertain whether the gmA was in the desired channel configuration. Figure 1 is a CD spectrum of a sonicated dispersion of DMPC/gmA in the presence of ferrous chloride. The spectrum is characteristic of the channel forming b-helical conformation, with positive extrema at 218 and 235 nm, a weak negative inflection at 229 nm and negative ellipticity below 208 nm.<sup>4c, 9</sup> Having confirmed the formation of ion channels in vesicles, the precipitation of iron oxides was carried out by the addition of NaOH till the pH of the solution was  $\sim 12$  (from an initial pH of  $\sim 4$  for the ferrous chloride vesicular solution). Compared to the slow development of a pale yellow coloration in pure DMPC vesicles, there was an almost instantaneous pale yellow color in the case of DMPC/gmA vesicles. That the gmA was still in the channel conformation was established by recording the CD spectrum. As can be seen from Figure 1, the spectrum was essentially unchanged confirming that the peptide was still present as a channel.

The characterization of the intravesicular precipitates was carried out by TEM investigations. Particles  $\sim 100$  Å in diameter were formed in DMPC vesicles, however, the particle size in DMPC/gmA vesicles was much smaller (30-40 Å), as seen in Figure 2. EDAX analysis was used to confirm that the particles were iron-oxides (Figure 2). This difference in size can be attributed to the faster efflux (a quicker pH jump) of protons out of the ion channels in DMPC/gmA, leading to faster and hence smaller particle formation due to enhanced nucleation rates. It is interesting to note that a 0.1 M  $\text{FeCl}_2$  solution (as used in these experiments) should in principle yield particles only 25 Å in size. As described by Mann, the formation of larger crystallites could be attributed to saturation binding of Fe to headgroup sites, leading to much higher effective concentrations of intravesicular Fe.<sup>6a</sup>

To investigate whether the presence of ion channels caused any differences in the phases of iron-oxides obtained, electron diffraction techniques were employed. Powder electron diffraction patterns for the iron-oxide particles for DMPC and DMPC/gmA systems are shown in Figure 3. Analysis of the diffraction patterns revealed that the iron-oxide formed inside DMPC vesicles was maghemite and that inside DMPC/gmA was magnetite. Maghemite is the oxidized form of magnetite, in which the cubic structure is preserved and the increased positive charge is accommodated by the ejection of 11% Fe creating

vacancies ( $f$ ):  $\text{Fe}_3\text{O}_4 \approx \text{Fe}_{2.67f0.33}\text{O}_4$ .<sup>11</sup> This leads to the appearance of additional lines in the diffraction pattern. The presence of lines at  $d = 2.63 \text{ \AA}$  and  $3.40 \text{ \AA}$  confirms that the iron oxide obtained in DMPC vesicles is indeed maghemite. No additional lines were observed in the magnetite derived from DMPC/gmA vesicles.

The differences in the iron oxides obtained can be rationalized in terms of the faster formation of iron oxide in gmA doped vesicles, due to highly enhanced proton transfer rates. Consequently, the degree of oxidation (*ferrous* ions are initially present) is lower and magnetite is formed. Without gm A ion channels, the slow diffusion of  $\text{OH}^-$  ions into the vesicles occurs with proportionately greater oxidation to *ferric* ions, leading to the formation of maghemite.<sup>12</sup> It might be possible to obtain magnetite in DMPC vesicles by control of the oxygen content in the surrounding atmosphere, but in the experiments described no such efforts were made.

We have described preliminary results obtained by using ion channels to control the phase and size of intravesicular crystallites. Our results indicate that the ion channels are functional. Additionally, they are able to modify the size and type of iron oxide crystals obtained. Control of particle size has important implications in materials science due to quantum size effects being manifested in colloidal particles.<sup>1a</sup> Besides, ion channels may render accessible novel mineral phases. The onset and control of mineralization in biological systems is a fascinating area of research and it is tempting to speculate that ion-channels are involved in those complicated signal transduction processes.

## References and Notes

### Part I

- (1) (a) Mann, S.; Webb, J.; Williams, R. J. P. Eds. *Biom mineralization: Chemical and Biochemical Perspectives* VCH Publishers, New York, 1989. (b) Sarikaya, M.; Aksay, I. A. Eds. *Biomimetics: Design and Processing of Materials* AIP Press, Woodbury, New York, 1995.
- (2) Addadi, L.; Moradian, J.; Shay, E.; Maroudas, N. G.; Weiner, S. *Proc. Natl. Acad. Sci. (U. S. A.)* **1987**, *84*, 2732.
- (3) Landau, E. M.; Popovitz-Biro, R.; Levanon, N.; Leiserovitz, L.; Lahav, M.; Sagiv, J. *J. Mol. Cryst. Liq. Cryst.* **1986**, *134*, 323.
- (4) (a) Borowitzka, M. A. *CRC Crit. Rev. Pl. Sci.* **1987**, *6*, 1. (b) Weiner, S. *J. Exp. Zool.* **1985**, *234*, 7.
- (c) Borman, A. H.; de Jong, E. W.; Huizinga, M.; Kok, D. J.; Westbroek, P.; Bosch, L. *Eur. J. Biochem.* **1982**, *129*, 179.
- (5) Addadi, L.; Weiner, S. *Proc. Natl. Acad. Sci.* **1985**, *82*, 4110.
- (6) (a) Rajam, S.; Heywood, B. R.; Walker, J. B. A.; Mann, S.; Davey, R. J.; Birchall, J. D. *J. Chem. Soc. Faraday Trans.* **1991**, *87*, 727. (b) Heywood, B. R.; Rajam, S.; Mann, J. *Chem. Soc. Faraday Trans.* **1991**, *87*, 735.
- (7) Berman, A.; Ahn, D. J.; Lio, A.; Salmeron, M.; Reichert, A.; Charych, D. *Science*, **1995**, *269*, 515.
- (8) (a) Groves, J. T.; Fate, G. F.; Lahiri, J. *J. Am. Chem. Soc.* **1994**, *116*, 5477. (b) Lahiri, J.; Fate, G. F.; Ungashe, S. B.; Groves, J. T. *J. Am. Chem. Soc.* Submitted.
- (9) m-Oxo dimer formation is facilitated in LB monolayers, see Hopf, F. R.; Möbius, D.; Whitten, D. G. *J. Am. Chem. Soc.* **1975**, *98*, 1584. We obtained UV spectra of the porphyrin by deposition on a glass cover slip, using a subphase of TRIS buffer (pH 6.3) containing 9 mM  $\text{CaCl}_2$ , at a constant surface pressure of 22 mN/m. The quality of the deposition was poor, and hence only the Soret band was clearly discernible in the UV spectrum, with an absorbance maximum at 422 nm. This value is closer to the Soret absorbance maximum for the iron m-oxo dimer of sulfonated tetraphenyl porphyrins (415 nm), as versus the monomer which had its maximum at 392 nm. See Fleischer, E. B.; Palmer, J. M.; Srivastava, T. S.; Chatterjee, A. *J. Am. Chem. Soc.* **1971**, *93*, 3162.
- (10)  $\text{CO}_2$  gas was bubbled through a stirred suspension of aqueous  $\text{CaCO}_3$ , for ~ 1 h. The suspension was then filtered, and  $\text{CO}_2$  gas was bubbled through the filtrate for ~ 1/2 h. Bubbling the gas for longer periods of time did not change the Ca concentration (as estimated by EDTA titrations) significantly.

(11) Bull, R. A.; Bulkowski, J. E. *J. Colloid and Interface Sci.* **1983**, *92*, 1. Based on structural data, tetraphenylporphyrins lying flat at the air water interface should occupy  $\sim 160 \text{ \AA}^2/\text{molecule}$ . Also see Hann, R. A. in *Langmuir-Blodgett Films* pp 59 - 67, Roberts, G. Ed. Plenum Press, New York, 1990.

We observed a drop in the surface pressure by  $\sim 5 \text{ mN/m}$  after the initial compression of the monolayer over the bicarbonate subphase. This could be attributed to a closer approach of the porphyrinic lipids due to dimer formation and/or changes due to  $\text{Ca}^{2+}$  nucleation.

(12) The results obtained using stearic acid monolayers were consistent with Mann's observations. We however observed calcite crystals (after  $\sim 8\text{-}10 \text{ h}$ ) that were exclusively triangular in projection, labeled as 'Type II' crystals<sup>6</sup>, as shown in Figure 2c. These crystals were transformed into the 'Type I' crystals<sup>6</sup>, with 4-edged basal planes, over a period of 4 - 5 days, as shown in Figure 2d. Viewed from the underside these crystals had smooth rhombohedral  $\{10\cdot4\}$  faces, often with central cavities. These cavities occurred ONLY on the underside, and have been attributed to diffusion limited growth caused by high supersaturation gradients, accompanying  $\text{CO}_2$  loss at the interface.

(13) SEM stage tilting experiments revealed an angle of  $\sim 17^\circ$  between each plane comprising the truncated corner and the adjacent  $\{10\cdot4\}$  face. This would correspond to a  $\{10\cdot2\}$  plane, based on the known crystal structure of calcite. All of the 15-20 crystals surveyed with the broken corners had this angular relationship.

(14) The cartoon for the m-oxo dimer 1 was constructed from the crystal structure of m-Oxo-bis[(5, 10, 15, 20-tetraphenylporphyrinato)iron(III)], see Swepston P. N.; Ibers, J. A. *Acta. Cryst.* **1985**, *C41*, 673. We also investigated the growth of  $\text{CaCO}_3$  crystals under monomeric tricarboxy amphiphilic porphyrins (free-base). The calcite crystals obtained were essentially similar with broken corners and cavities on opposite  $\{10\cdot4\}$  faces. However, the corners had undelineated facets and were more flat, and on average much were larger in size. It has been suggested that free base porphyrins readily form dimeric sites even where no covalent bond formation occurs, and hence the nucleation mechanism is expected to be similar.<sup>9</sup>

## Part II

(1) (a) *Biomimetics: Design and Processing of Materials*, Sarikaya, M.; Aksay, I. L. Eds. AIP Press, New York, 1995. (b) *Biomimetalization: Chemical and Biochemical Perspectives*, Mann, S.; Webb, J.; Williams, R. J. P. Eds. VCH Publishers, 1989.

(2) Frankel, R. B.; Bazylnski, D. A. in *Biomimetics: Design and Processing of Materials*, Sarikaya, M.; Aksay, I. L. Eds. pp 199 -215 and references contained therein, AIP Press, New York, 1995.

(3) For reviews on ion channels see: Yagi, K.; Pullman, B. *Ion Transport Through Membranes*, Academic, Florida, 1987.

(4) (a) Katz, E.; Demain, A. L. *Bacteriol. Rev.*, **1977**, *41*, 449. (b) Urry, D. W.; Goodal, M. C.; Glickson, J. D.; Mayers, D. F.; *Proc. Natl. Acad. Sci. U. S. A.* **1971**, *68*, 1907. (c) Urry, D. W.; Trapane, T. L.; Prasad, K. U. *Science*, **1983**, *221*, 1064.

(5) Myers, V. B.; Haydon, D. A. *Biochim. Biophys. Acta* **1972**, *27*, 313.

(6) (a) Mann, S.; Hannington J. P.; Williams, R. J. P. *Nature*, **1986**, *324*, 565. (b) Youn, H-C.; Baral, S.; Fendler, J. H. *J. Phys. Chem.* **1989**, *92*, 6320. (c) Heywood, B. R.; Eanes, E. D. *Calcif. Tissue. Int.* **1987**, *41*, 192.

(7) Vesicles are widely used as membrane mimetic systems. In our laboratories, we have carried out catalysis and multi-heme self assembly in phospholipid vesicles. See: (a) Groves, J. T.; Neumann, R. *J. Am. Chem. Soc.* **1989**, *111*, 2900. (b) Groves, J. T.; Ungashe, S. B. *J. Am. Chem. Soc.* **1990**, *112*, 7796. (c) Groves, J. T.; Fate, G. F.; Lahiri, J. *J. Am. Chem. Soc.* **1994**, *116*, 5477.

(8) Liu, H.; Graff, G. L.; Hyde, M.; Sarikaya, M.; Aksay, I. A. *Mat. Res. Soc. Symp. Proc.* **1991**, *218*, 115.

(9) A DMPC:gmA ratio of 25:1 was used. During the sonication of the DMPC/gmA, the lipid mixture was immersed in a water bath at  $\sim 45^\circ\text{C}$ . Sonication of pure DMPC was carried out at room temperature. The conformation adopted by gmA in the membrane is dependent on its conformational behavior in the original organic solvent. TFE is the recommended solvent because the gm adopts the correct b-helical conformation in TFE and in the membrane, following solvent removal and rehydration. See Killian, J. A.; Prasad, K. U.; Hains, Urry, D. W. *Biochemistry*, **1988**, *27*, 4848.

(10) Bio-Rad AG 50W-X2 ( $\text{Na}^+$  form) resin was used for cation exchange. A spectrophotometric flow cell was attached to the outlet of the column, and the elution profile was monitored spectroscopically for lipid and peptide absorbances. The flow cell was connected to a fraction collector and fractions containing the lipid and lipid/gmA were used for the mineralization experiments.

(11) Schwertmann, U.; Cornell, R. M. *Iron Oxides in the Laboratory: Preparation and Characterization* VCH Publishers, Weinheim and New York, 1991.

(12) At a peptide : lipid ratio of 1:25, there are  $\sim 75$  channels per vesicle. In the DMPC/gmA vesicles, NaOH addition raises the intravesicular pH instantaneously, such that the  $\text{Fe}^{3+}/\text{Fe}^{2+}$  ratio is determined only by the  $\text{Fe}^{2+}$  ions that have already been oxidized to  $\text{Fe}^{3+}$  prior to alkali addition. Consequently, the  $\text{Fe}^{3+}/\text{Fe}^{2+}$  ratio is lower in DMPC/gmA than in pure DMPC. Under the time frame of the experiment (from making a fresh ferrous chloride solution to carrying out the pH jump), typically  $\sim 45$  min, the balance between the  $\text{Fe}^{3+}/\text{Fe}^{2+}$  ratio and pH rise probably determines the formation of magnetite in DMPC/gmA vesicles. In pure DMPC, after alkali addition, there is simultaneous oxidation and slow  $\text{OH}^-$  influx, and thus maghemite (with a higher  $\text{Fe}^{3+}$  content) gets formed. The variation in iron oxide formation at different ratios of gmA/DMPC is currently being pursued.